ELSEVIER

Colloids and Surfaces A: Physicochem. Eng. Aspects xxx (2005) xxx–xxx

COLLOIDS AND SURFACES A

www.elsevier.com/locate/colsurfa

Protein and surfactant foams: linear rheology and dilatancy effect

S.P.L. Marze, A. Saint-Jalmes *, D. Langevin

Laboratoire de Physique des Solides, Université Paris-Sud, Bat. 510, 91405 Orsay Cedex, France

Received 4 October 2004; accepted 21 January 2005

Abstract

We report results on the dependence of foam rheology on the nature of its components (gas, liquid and surfactant). We have varied the liquid bulk properties, the gas–liquid interfacial properties, which implies also different thin liquid films properties, and the gas. Microscopic characterizations are also performed to find correlations between the different length scales, and to interpret the macroscopic rheological behavior (oscillations and creep). We have found that the elastic modulus G', once normalized by the Laplace pressure, does not depend on the foam components, whereas the loss modulus G'' shows some dependence with the interfacial properties. We show that the gas is an important factor for these moduli because of its role in the foam aging, via coarsening. We have also evidenced a dilatancy effect taking place under continuous shear, by using a special foam sample shape, in which only a foam band is subjected to shear. We have observed and measured an increase of the liquid volume fraction ε in that band.

Keywords: Foam; Rheology; Interface; Coarsening; Dilatancy

1. Introduction

An aqueous foam can support small shear forces as a solid [1,2]. The elastic behavior comes from the distortion and the packing of the bubbles in the foam, meaning that an osmotic pressure is actually exerted on the bubbles and that some surface energy is stored in their interfaces. Applying a shear deformation creates additional surface area and gives rise to a restoring force, hence an elastic modulus. The scale of this modulus is set by the pressure, σ/R', where σ is the gas–liquid surface tension and R' an average bubble dimension (more precisely, simulations tend to show that the relevant quantity is the Sauter mean radius R_{32} – the ratio between the third and the second moments of the size distribution – rather than the mean radius R [2,3]). Both theoretical [3–13] and experimental works (often done on emulsions) [14–20] have been performed in order to elucidate the dependence of the shear modulus with the different parameters, especially the liquid fraction ε (or the gas fraction, ϕ, with $\phi = 1 - \varepsilon$). This parameter ε (or ϕ) describes the amount of packing and distortion of the bubbles. While the theoretical works mainly deal with the limit of the perfectly dry foam ($\phi = 1$) and with 2D systems, experimental results on 3D foams and emulsions seem to show that there is a simple scaling law for the elastic modulus, depending only on the liquid fraction, once the surface tension and the bubble size are taken into account (though it is still not clear if the modulus scales with R or R_{32}, which can be slightly different in the case of polydisperse systems) [14–16,20].

However, recent experiments with emulsions (stabilized by proteins, or solid particles [21–23]) show unexpectedly high values of the elastic modulus, which can be up to 30 times bigger than what the scaling law predicts (and which definitively cannot be explained by differences between R and R_{32}). An important issue is thus to know if these same unexpected high values can also be found for foams, and if so what are their origins. This means one has to figure out which new parameters have to be added to explain the complete elastic behavior. For foams, it is often found that the macroscopic behavior is the result of different coupled effects acting at all the internal length scales. For instance,

* Corresponding author. Tel.: +33 1 69 15 69 60; fax: +33 1 69 15 60 86.
E-mail address: saint-jalmes@lps.u-psud.fr (A. Saint-Jalmes).

0927-7757/$ – see front matter © 2005 Elsevier B.V. All rights reserved.
doi:10.1016/j.colsurfa.2005.01.014

regarding foam drainage, recent results have shown that one has to include in the data interpretation the surface shear viscosity, a non-trivial ingredient related to the microscopic scale of the gas–liquid interface [24–25].

In a more general view, it is important to understand how the whole rheology (both in terms of elastic, loss moduli and steady flow properties) depends on the microscopic parameters, and thus on the foam components (surfactant, liquid and gas). Changing the surfactants has an impact not only on the surface tension σ, but also on the gas–liquid interfacial properties (both the dilatational and shear contributions). The nature of the surfactant also modifies the properties of the thin liquid films which separate the bubbles. The bulk liquid characteristics (shear or elongational viscosities, possible dependence on the shear rate) may also be important parameters, as well as the properties of the gas. Above a yield stress [1], foams flow irreversibly: here again, it is important to determine if the foam components may play a role on the flow properties as the viscosity, on the type of flow (uniformity of shear, or shear localization, wall slip, etc.).

In this paper, we report rheological studies and comparisons between foams having well-characterized and different microscopic properties. We also report results on the shear localization issues and give evidences of a dilatancy effect occurring in foams.

2. Materials, samples and microscopic characterization

We have selected two different types of surface-active agents, in order to obtain foams for which the interfacial and thin film behaviors are different. In one hand, we used a small classical surfactant, SDS (sodium dodecyl sulfate), and in the other hand we used casein (the principal milk protein, and which can be considered as a long random copolymer). Both chemicals are purchased from Sigma, and used as received. For the pure SDS and casein solutions, the concentrations used are, respectively, $c_{sds} = 6$ g/L and $c_{cas} = 4.5$ g/L. The later is brought at pH 5.6 by adding a phosphate buffer at 10 mM, and then placed in an ultrasonic bath for 30 min, so as to prevent casein from aggregating during the dissolution. We also prepared SDS/casein mixture solutions, where the casein concentration is fixed at $c_{cas} = 4.5$ g/L, and the amount of SDS added is varied from 0.3 to 3 g/L.

The casein molecules adsorb at the gas/solution interfaces, and form much more elastic and rigid surfaces than the SDS ones [26,27]. Also, the thin liquid films are quite different [28–30]: flat, homogeneous and very thin for SDS (as for usual surfactant, with typical thickness of a few tens of nm), while the films are thick for casein, with aggregates confined in a jellified matrix, making the film quite non-uniform in texture and thickness. Typical mean thickness for these casein films is of the order of a few hundreds of nanometers [29,30].

Beside the different surface-active agents, a polyacrylic branched homopolymer – Carbopol 911 from BF/Goodrich – is used as a bulk viscosifier. Carbopol is used as received, added to a SDS solution at $c_{SDS} = 6$ g/L, with concentrations ranging from 0.5 to 3 g/L. The resulting solutions are slightly shear thinning, and for a typical shear rate of $1\,s^{-1}$, the bulk viscosity varies from 1 to 10^3 mPa s. Note that the pure aqueous Carbopol solutions have much higher viscosities and stronger shear-thinning behavior than the mixtures: there is a strong complexation in bulk of SDS and Carbopol providing a change in the microstructure of the Carbopol microgels. However, at the interfaces, the presence of Carbopol has only a tiny effect, at any concentrations (evidenced by surface tensions lowered by 1 or 2 mN/m, and by a similar increase of the interfacial viscoelastic moduli). Thus the addition of Carbopol has only small effects on the interfaces and on the thin films, but strongly changes the bulk liquid viscosity (contained in the network of Plateau Borders and nodes [1]).

For the gas, we used nitrogen N_2 and hexafluoroethane C_2F_6: the fluorinated gas has much lower diffusion and solubility constants. The characteristic coarsening time t_c, as defined in [31], is given by $t_c = d_0^2 h/2K_{geo}K_{gas}\gamma\ f(\varepsilon)$, with K_{geo} is a geometrical constant (reflecting the bubble geometry), K_{gas} a gas constant (including the diffusivity and solubility constant), $f(\varepsilon)$ a function of the liquid content, h the thin film thickness, d_0 the initial mean bubble diameter and γ the surface tension. Experimentally, we have measured that the typical coarsening times for an SDS foam are 150 s with N_2 and 4500 s with C_2F_6, at a constant liquid fraction of $\varepsilon = 0.15$ [28,30].

The foams are produced by a home-made apparatus called the turbulent mixer, and described in [32], allowing to make homogeneous foams of any desired liquid fractions between 0.03 to 0.3. The mean bubble diameter (initially, just after the foam production), measured by microscopy at the surface of a 3D sample, is 0.10 mm for pure casein foam, and tends to be a bit larger for pure SDS foam (up to 0.14 mm). Note that the foams are polydisperse [32], and that the polydispersity and the initial mean bubble size do not depend on the gas used. For all the foams studied here, even if the mean bubble sizes can be a bit different, the size distributions of all these foams strongly overlap: there are basically no very small ($D < 0.04$ mm), nor very large bubbles ($D > 0.25$ mm).

For each solution the surface tension is measured using the drop method (here, in the inversed configuration, with a rising bubble immerged in the solution). For a protein solution at low concentrations, slow adsorption dynamics are usually observed, with no final equilibrium value (the surface tension always decreases with time). However, for the high casein concentrations used here, the adsorption is relatively fast and the surface tensions do not vary more than 5% between the initial value, and a plateau value obtained after a few minutes. We thus use here a typical value found after 3 min. This gives $\sigma = 46$ mN/m for pure casein, $\sigma = 36$ mN/m for pure SDS, and intermediate values for the mixtures (note that the addition of a small amount of SDS, 0.05 g/L, already drops the surface tension down to $\sigma = 40$ mN/m). It thus turns out that the

surface tension is a parameter that does not vary much with the interfacial components. The same bubble method is used to measure the interfacial viscoelastic properties of the interfaces (via controlled oscillation of the bubble volume). Note that such measurements only reflect the intrinsic elastic and viscous effects within the air–liquid interface, and not within a thin liquid film. In all the cases, the dilatational elastic modulus ε_r is a few times higher than the viscous one, ε_i. As expected, both moduli are maximum for the interfaces covered by caseins ($\varepsilon_r \approx 10+/-0.2$ mN/m and $\varepsilon_i \approx 2.5+/-0.3$ mN/m, after 3 min of adsorption). Adding SDS (in the concentration range investigated here) reduces continuously these moduli down to $1.5+/-0.3$ mN/m ($\varepsilon_r \approx 1.9+/-0.3$ mN/m and $\varepsilon_i \approx 0.7+/-0.3$ mN/m, for the pure SDS). Note finally that the viscoelastic properties of these interfaces depend on the frequency, and that here the measurements are made at 0.1 Hz.

3. Macroscopic rheological experiments: small deformations and linear regime

The rheological measurements are done with a rheometer MCR 300 from Paar Physica. For the liquid solutions, a Couette cell with a double gap is used. For foams, the measurement device is a homemade cone-plate system, machined from bulk Plexiglas, and cover with sand grains to avoid slips at the walls. The cone angle is 10° and both cone and plate have a diameter of 175 mm. The foam is directly injected from the turbulent mixer inside the cell, from the center of the bottom plate, and the cell is filled with no gap or holes in a few seconds.

Amplitude sweep experiments (oscillations at a fixed frequency $\omega = 1\,\mathrm{rad\,s^{-1}}$ and with a strain amplitude γ varied from 10^{-4} to 1) allow to measure the storage and loss moduli (G' and G''), and to determine the range of linear response and the foam yielding [33]. Creep experiments have also been performed: the foam is subjected to a constant stress Σ and the resulting strain γ, and compliance J ($J = \gamma/\Sigma$) [33], are measured versus time.

We first performed some amplitude sweep measurements with a simple surfactant (SDS) foam, made with C_2F_6 (to reduce coarsening as much as possible). We have recovered the classical curves for G' and G'' as a function of the strain [14,15,20]: at low strains, plateau value for G' (named G'_0 in the following), and almost no variations for G'' (also allowing to define a strain-independent value G''_0); and at high strains, both moduli decreases drastically, as a signature of the foam yielding (the yield strain and stresses, defined as the values for which the relation between stress and strain is no longer linear, occurs slightly before the bump in G'' [20]). Our results are consistent with previous ones on foams [17–20]. Moreover, when the liquid fraction ε is varied, we find a dependence of $G'_0/(\sigma/R)$ which follows the previously found law (expressed more practically with the gas fraction ϕ, $G'_0/(\sigma/R) \sim \phi(\phi - \phi_c)$ [14–15]). Note that the whole range of liquid fraction cannot be thoroughly studied on ground due to drainage effects, only rather fast measurements can be performed on fresh foams (within the first minutes after the production). In order to test the effect of the foam components on G' and G'', the liquid fraction is fixed in the following at an intermediate value $\varepsilon = 0.15$, corresponding to a good compromise for which neither drainage or coarsening are too quick.

3.1. Bulk viscosity effects on viscoelastic moduli

Experiments with the different amount of Carbopol added to a surfactant solution clearly show that a same elastic modulus G' (with $G'_0 = 140$ Pa) is perfectly recovered for all the bulk viscosities. The loss modulus shows a slight increase with the bulk viscosity, but it varies only by a few percents whereas the bulk viscosity is varied by more than three orders of magnitude. It thus appears that the linear viscoelastic properties of foams are almost independent of the bulk viscosity (at least in the range studied here, which covers the typical liquid viscosities used in most industrial applications).

3.2. Interfacial effects on viscoelastic moduli

The viscoelastic moduli of SDS, casein and SDS/casein mixtures foams are displayed on the Fig. 1 (foams made with C_2F_6, and at $\varepsilon = 0.15$). We first discuss the behavior of G'. For all the foams, the amplitude sweep curves keep the same classical shape with only small variations for the plateau values G'_0. A more accurate comparison between the different foams can be done once G'_0 is normalized by the Laplace pressure σ/R (here, we choose R as the mean bubble radius) [14,15]. In Fig. 2, $G'_0/(\sigma/R)$ is plotted as a function of the amount of SDS added in the casein solution, together with values found at the same liquid volume fraction in other studies on emul-

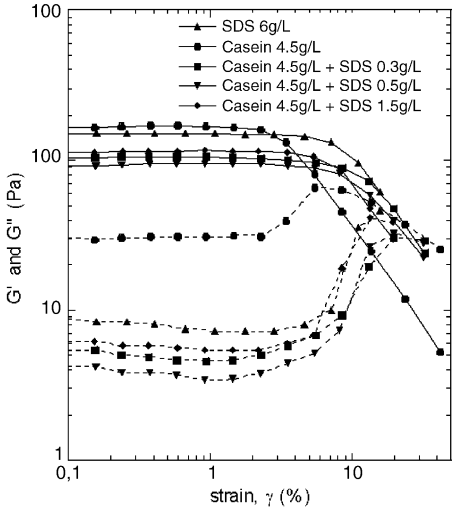

Fig. 1. G' (full lines) and G'' (dotted lines) as a function of the applied strain γ, for various C_2F_6 foams, with initial liquid fractions of 0.15, and at a fixed frequency $\omega = 1\,\mathrm{rad\,s^{-1}}$.

sions stabilized either by surfactants (PDMS silicone oil in water with SDS at 10 mM [14]), proteins (hexadecane oil in water with bovine serum albumin [21], soybean oil in water with sodium caseinate as a stabilizer [22]), or solid particles (PDMS silicone oil in water with partially hydrophobized silica particles [23]). The value found for our pure SDS foams is indicated by a dedicated symbol and the arrow, and the dashed line corresponds to $G'_0/(\sigma/R) = 0.25$, which is the measured value for surfactant monodisperse emulsions at $\varepsilon = 0.15$ [14].

For our foams, $G'_0/(\sigma/R)$ turns out to be almost constant and independent of the chemicals used: no huge differences are found between protein and surfactant foams, in opposition to results for emulsions. Moreover, for all our measurements the ratio $G'_0/(\sigma/R)$ is very close to 0.25. In fact, and in contrary to emulsions, we have found that the normalized moduli for the protein foams and mixtures are even a bit smaller than the expected value (especially for the mixtures). It is difficult to know if this is a significant effect, or if it may come from the normalization by σ/R: with possible different in situ surface tension, for instance; or in relation with the scaling by R rather than by the radius R_{32}. Note, however, that we believe that the ratio R/R_{32} is constant for all our foams (since from microscopic observations the polydispersity is not changing): thus the relative evolution seen in Fig. 2 as SDS is added is meaningful, and remains the same whatever the radius used in the scaling. Physically, a smaller value of $G'_0/(\sigma/R)$, for a given liquid fraction, could also come from a lower effective compaction. So it turns out that for the casein foams we have not found unexpectedly high elastic modulus as for protein emulsions: the surface tension in foams remains actually much too high (and higher than in emulsions) so that all other elastic contributions from the interfaces are comparatively smaller and hidden. In fact, also for emulsions stabilized by casein molecules, moduli in

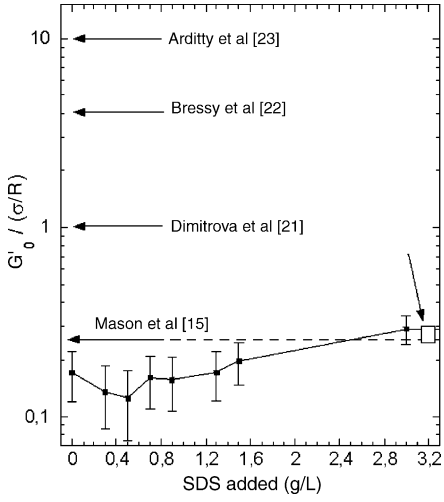

Fig. 2. G'_0 normalized by the Laplace pressure (σ/R) as a function of the amount of SDS added in a pure casein solution. Arrows represent results from other studies, all at $\varepsilon = 0.15$. The arrow and the open square on the right, stand for the pure SDS value.

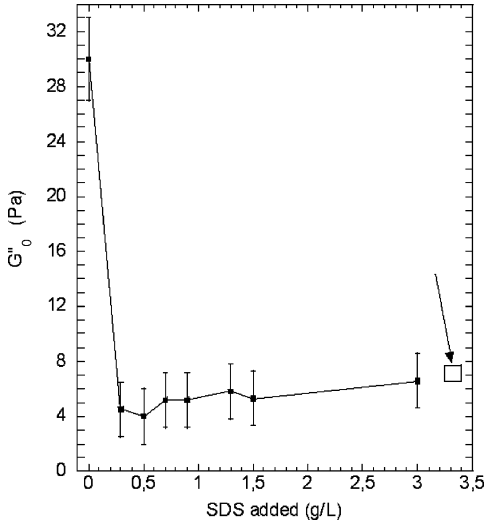

Fig. 3. G''_0 as a function of the amount of SDS added in a pure casein solution. The arrow and the open square stand for the pure SDS value (all foams at $\varepsilon = 0.15$).

agreement or not with the scaling law have been found, depending on the oil used, thus on the oil–water surface tensions [21,22].

The behavior of the loss moduli G''_0 is reported in Fig. 3 (without any normalization). Here some significant differences are found between the pure casein foams and the surfactant ones: G''_0 is roughly 4–5 times bigger for the casein foams than for the SDS ones. Nevertheless, as soon as a small amount of SDS is added, the modulus decreases down to the value obtained for a pure SDS foam (indicated by the arrow on the right). It thus seems that some extra dissipation occurs for the protein foams either coming from the viscous contributions within the interfaces and/or from the thin films (with their thick and jellified texture, and confined aggregates). Note here again that, for the mixtures, a same trend as for G'_0 is observed: for both moduli, a minimum is found for the intermediate mixtures, showing that the mixing is probably not a simple process, which does not follow a simple linear curve between the two limits.

Note that our measurements were made at a constant frequency, $\omega = 1\,\mathrm{rad\,s^{-1}}$. However, the viscoelastic moduli depend on a complex manner on that frequency [18–20,34]. For every foam, there is nevertheless always a range of intermediate frequencies ω (here for our systems, typically from 0.1 to $5\,\mathrm{rad\,s^{-1}}$) where the moduli are almost frequency-independent, and it is inside this range that we have performed our measurements. So the results discussed here are representative of that regime, and it is thus meaningful to compare them. Studies and comparisons at all frequencies is an ongoing work (the low-frequency range is partially studied in Section 3.4). As another remark, we also want to point out that for the casein foams, even though the $G'_0/(\sigma/R)$ is identical to the one for SDS foams, the yielding seems to be slightly different (the yield strain is smaller, Fig. 1), and this remains to be completely explained.

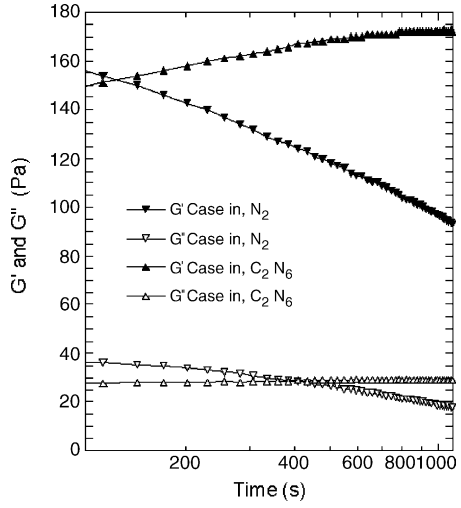

Fig. 4. G' and G'', measured at fixed frequency $\omega = 1\,\mathrm{rad\,s^{-1}}$ and strain $\gamma = 0.005$, as a function of the foam age. Casein foams with different gases, at $\varepsilon = 0.15$.

3.3. Gas effects on viscoelastic moduli

To investigate the effect of the gas, we studied pure casein foams, made either of C_2F_6 or N_2. Within the linear regime (constant strain of 0.5% and $\omega = 1\,\mathrm{rad\,s^{-1}}$), we have measured the viscoelastic properties, as well as their time evolution (Fig. 4). At time zero, the elastic modulus is almost independent of the gas used (small variations may come from different initial bubble sizes). Initially, the loss modulus depends slightly on the gas, and the observed variations are up to now difficult to understand. Non-aging materials would give constant values for G' and G'' over time. Foams are however out of equilibrium systems, and age mainly via drainage and coarsening. Both phenomena are expected to affect the elastic properties as they respectively change the liquid fraction and the bubble size. Regarding G', two opposite behaviors are indeed found. For C_2F_6, we know that almost no coarsening occurs (for casein, the coarsening time at constant $\varepsilon = 0.15$ is $t_c \approx 2 \times 10^4$ s [28,30]). However the foam drains: as the foam gets dryer in a large part of the sample, the bubbles get more packed and the modulus increases. The decrease of G'_0 for N_2 is explained by the opposite situation: the domination of coarsening (the coarsening time at constant $\varepsilon = 15\%$ is $t_c \approx 850$ s [28,30]) over drainage. Obviously, both effects occur in the foam as they are always coupled: here, variations of the bubble size due to coarsening (which is moreover enhanced as the foam drains) are larger that liquid fraction ones due to drainage. So, changing the gas allows to change the balance between drainage and coarsening times and thus the time evolution of the foam rheological measurements.

For G''_0, the same dynamical behaviors are observed as the gas is changed. This is especially interesting for the case with N_2: this means that G''_0 may depends the same way as G'_0 on the foam aging, and thus on bubble size. One could then even wonder if G''_0 could be also scaled by a simple pressure term σ/R', as reported for emulsions systems in [16] and for foams in [19] (though this remains surprising as such Laplace pressure should only be relevant for describing the elastic contribution).

3.4. Creep measurements

Creep experiments allow a complementary study of the interfaces and gas contributions to foam linear rheology [33,35]. Measurements of the compliance $J(t)$, linked to those of $G^*(\omega)$ by a Laplace transform [33], can be used to verify and implement the oscillatory measurements. Here, we only present preliminary creep results and qualitative analysis. The complete quantitative and comparative analysis of the creep experiments, in terms of fitting parameters as a function of the foam parameters – liquid fraction, nature of the gas and surfactant – as well as the relation between these results and the interfacial viscoelasticity [35,36] is under progress, and will be reported in a future dedicated article. Creep curves are presented in the Fig. 5 for foams made of different combinations of gas and interfacial components. All the curves share the same shape: a first instantaneous increase is followed by a curved transient part, and then a final regime with a linear slope is observed (corresponding to a steady-state deformation). Actually, such creep curves, as proposed for the first time in [35], can be fitted throughout the available experimental times, by a relationship $J(t) = 1/G_0 + 1/G_1(1 - \exp(G_1 t/\eta_1)) + t/\eta_0$, where the three terms, respectively, represent the three parts of the curves describes above. For a fixed gas (C_2F_6), we have found that the variation of the interfacial properties (SDS or casein) slightly changes the exponential parameters G_1 and η_1, and the associated characteristic timescale $\tau_1 = \eta_1/G_1$ (of the order of 10–20 s). For the casein foams, this decay is indeed a bit slower, indicating more viscous dissipative contributions, and qualitatively confirming the differences seen for G'' between pure casein and SDS foams. At long times, the steady-state slope strongly depends on the gas used (Fig. 5). Such spe-

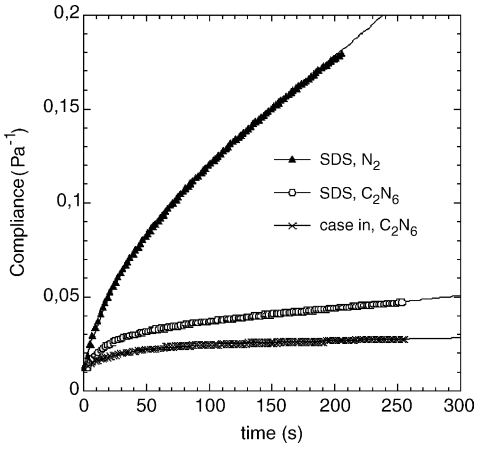

Fig. 5. Creep curves (compliance J vs. time) for three solution/gas couples, at $\varepsilon = 0.15$. Symbols represent the data, and the lines are the adjusted curves, as discussed in the text.

cific flow behaviors at long times are due to the coarsening process, as reported in [35], and in [34] (where relaxation experiments were performed). In fact, at long times, the stresses are relaxed by coarsening-induced events, and coarsening unjams the foam, which then flows like a classical liquid, at a viscosity η_0 depending on the gas [34,35]. Here we confirm these ideas, and find that the viscosity η_0 is indeed much bigger for the low coarsening foam (with C_2F_6) than for the fast coarsening one (with N_2). Moreover, we also evidence here the effect of the interfacial components on coarsening: a higher η_0 (meaning lower coarsening) is found for the casein foams (while keeping the same gas, C_2F_6). This can in fact be explained by the differences in the thin film thickness h: the coarsening times and rates are indeed directly proportional to h, and the difference of thickness between SDS and casein foams can be estimated around 5 [30]. Note finally that for the long times behavior, the linear slope is only valid for relatively short time period, and should not remain over long period of time, as the coarsening rate is actually not constant with time.

4. Steady flow and dilatancy effects

Foams can also be sheared continuously, at constant rates, providing measurements of viscosity and viscous stresses. The interpretation of the flow curves and comparisons between samples are only valid if the deformation is always well controlled and uniform. Recent results have shown that, for some cases and systems, shear localizations occur [37–39] resulting to shear bands in the samples. Previous measurements in foams however tend to show that the shear is uniform [40]. In addition to these non-uniform effects within the sample, the possibility of slip at the cell walls has also to be taken into account, and such effects also strongly affect the macroscopic rheological measurements. The difficulty to clarify these issues in 3D foams comes from the fact that the uniformity of the shear is not easy to test or to measure. The optical properties of foams only allow to follow the bubble motion at the edge of a sample.

We decided to investigate this problem of possible shear localization by a different way: creating on purpose a permanent and controlled shear localization inside a foam sample, and looking at its properties, and what this phenomenon implies. In order to localize the shear in a dedicated part of the foam, we have used a thick SDS foam sample (made with C_2F_6) confined and sheared between a fixed plate and a rotating one. At rest the sample has a hourglass shape, created by separating the plates from a smaller sample thickness (1 cm) up to the final one (7 cm). The smaller radius is then in the middle height (Fig. 6). Under rotation of the top plate, a thick part of foam turns as a solid body together with the top plate; while at the bottom, another thick part remains still. All the shear is then localized within an middle region of a few bubble thickness.

In the sheared region, visual observations show that the bubbles finally get a more spherical shape, different from the quite packed and polyhedral one of the upper and lower part. This also results in a different light reflection pattern (Fig. 6). This means that some liquid seems to be transported into the sheared band. Visually, the effect is rather fast and comes to an equilibrium situation after a few seconds. It is perfectly reproducible, and even perfectly reversible: when the rotation stops, the foam gets back to its initial state, with no more differences within the sample. Note that rather similar observations are reported in [41], though interpreted as

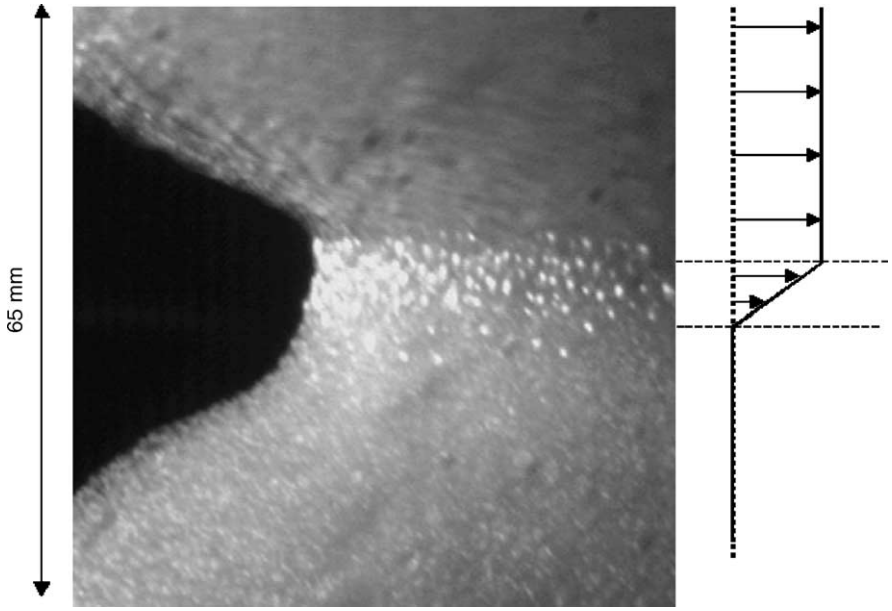

Fig. 6. Picture of the foam taken 17 s after the start of the top plate rotation and corresponding velocity profiles along the vertical axis. The shear only occurs in the central part, and this results in liquid transport and creation of a stable liquid fraction gradient (initial liquid fraction, $\varepsilon = 0.10$).

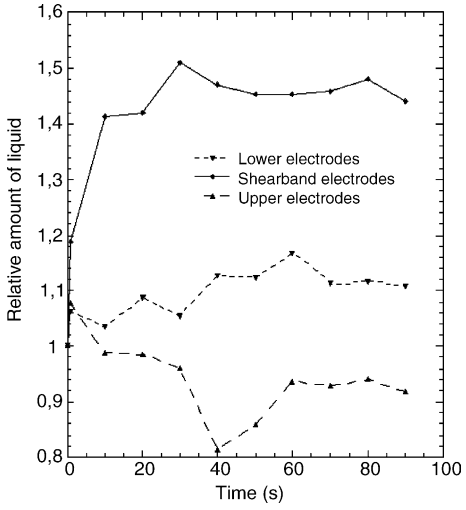

Fig. 7. Relative evolution of the amount of liquid within, below and above the controlled shear band, normalized by the value at $t = 0$ s (initial uniform liquid fraction, $\varepsilon = 0.07$).

a shear-induced size segregation. In fact, we can exclude this mechanism in our studies: our observations show this is the same bubbles which remain inside the central part (before, and during the shear). There are no exchanges or bubble shifts, evidencing that new bubbles with a different size may be brought inside the sheared part. Moreover, when the shear is stopped, the bubbles instantaneously stop, and as the liquid re-distributes evenly by capillarity inside the foam, the previously sheared bubbles finally look back exactly as the other unsheared ones (the visual observation and aspects of bubbles of equal volumes actually depends on the foam liquid fraction).

To verify the direct observations, we performed electrical conductimetry measurements at different positions in the foam [1]. Diametrically opposed couples of electrodes are placed at, below and above the shear band height. Normalized conductances, directly proportional to the liquid content, are reported in Fig. 7: the measurements confirm the liquid fraction increase in the sheared region. The first investigations show that this increase can be quite significant, and up to 50% when starting with a foam having a homogeneous liquid fraction of typically 0.1. Measurements on the two other electrodes show a constant value or a slight decrease, but not of the same amplitude of the increase in the sheared band: in this first setup, the electrodes were probably too close to the sheared part (a few bubbles apart), and the measurement is then made through both unsheared and sheared foam. More measurements, covering the whole foam height, are foreseen, and should provide us the time evolution of the liquid profile.

In the sheared region, bubbles must constantly change their relative positions. We have found that some liquid can be sucked into a sheared foam (from an unsheared contacting foam): this means that in this process of bubble motion and shear, the bubbles slightly move apart from each other, increasing their relative distance. This phenomenon is called dilatancy, meaning that a material increases its volume under shear. Though it is a well-known effect for granular materials, it has just recently been discussed in the framework of aqueous foams [43]. Note that here we are discussing about the dynamic dilatancy (or Bagnold's dilatancy [44]) corresponding to the case of continuous applied shear, and not in the quasistatic state.

The results tend to show that shear localization (or shear banding) and liquid gradients are strongly connected. As soon as the shear is not uniform, the liquid fraction could also becomes non-uniform, and this should also work in the opposite way, possibly evidencing a mechanism for the occurrence of shear localization (induced by liquid fraction heterogeneities).

It is also interesting to point out the link between dilatancy and the convective instabilities seen in the situation of forced drainage [44–45], as initially proposed in [42]. These instabilities create a paradoxical situation, not yet understood, where foam parts of different liquid fractions coexist within a same sample (in spite of capillarity effects which tend to homogenize the liquid distribution). We show here that such a situation is actually possible: in our sample, and due to dilatancy effects, foams of different liquid fraction indeed coexist, because each part is submitted to a different shear. The dilatancy suction counterbalance the capillary suction. As in the convective instabilities, the driest foam mostly moves as a solid body, with no internal shear, oppositely to the wettest part where more shear occurs.

5. Conclusions

The results reported here, on SDS, casein and SDS/casein foams at a fixed liquid fraction $\varepsilon = 15\%$, show that the elastic modulus G'_0 can be practically considered as independent on the foam chemical components (once normalized by the surface tension σ). Indeed, we have not found the same effect reported for protein emulsions with high surface viscoelasticity. The main reason for this difference is the too high surface tensions always present in foams: σ is always much bigger than any interfacial elasticities ε_r. However, the results show some effects of the chemicals on the loss moduli G'', which origin remains to be completely understood. If the gas does not change the initial rheology, it changes the time evolution of the foam mechanical properties via the foam aging, as the gas properties set the balance between drainage and coarsening. We have also confirmed the crucial role of coarsening in the long time (low frequency) regime. At long times, the foams flows as a simple liquid as the coarsening unjams the foam. We have also recovers, via the creep experiments, that the coarsening process can depend on the chemicals, via their effects on the thin film thickness. Concerning the steady-flow situation, we have found clear evidences of a dilatancy effect. One of the consequences of this effect is the unexpected cohabitation of wet and dry parts in a same foam, which can actually happens because these different parts are subjected

to different shears. We believe that this connection between liquid gradients and shear localization could be an important ingredient to understand both the occurrence of shear banding, and the mechanism of the convective instabilities.

The results reported here mainly concern foams at an initial liquid fraction of 0.15. As noted already in the text, it is strongly possible that different behaviors occur at other liquid fractions, especially in both limits of extremely dry and extremely wet foams. The continuation of this work (liquid fraction dependence, frequency dependence, use of other interfacial and bulk chemicals, studies on the yield point and above it, etc.) is under progress, and should help us in the future to better understand all the coupling between interfacial properties, aging and rheology.

Acknowledgements

This work has been supported in part by the Centre National d'Etudes Spatiales (CNES) and the European Space Agency (ESA).

References

[1] D. Weaire, S. Hutzler, The Physics of Foams, Oxford University Press, New York, 1999.
[2] H.M. Princen, The structure, mechanics and rheology of concentrated emulsions and fluid foams, in: Sjoblom (Ed.), Encyclopedic Handbook of Emulsion Technology, Marcel Dekker, New York, Basel, 2000 (Chapter 11).
[3] H.M. Princen, A.D. Kiss, J. Colloid Interf. Sci. 112 (1986) 427.
[4] H.M. Princen, J. Colloid Interf. Sci. 91 (1983) 160.
[5] D. Stamenovic, T.A. Wilson, J. Appl. Mech. 51 (1984) 229.
[6] S.A. Kahn, R.C. Armstrong, J. Non-Newtonian Fluid Mech. 22 (1986) 1.
[7] H.M. Princen, J. Colloid Interf. Sci. 91 (1986) 160.
[8] A.M. Kraynik, Annu. Rev. Fluid Mech. 20 (1988) 325.
[9] F. Bolton, D. Weaire, Phys. Rev. Lett. 65 (1990) 3449.
[10] D. Stamenovic, J. Colloid Interf. Sci. 145 (1991) 255.
[11] D.A. Reinelt, A.M. Kraynik, J. Fluid Mech. 311 (1996) 327.
[12] A.M. Kraynik, D.A. Reinelt, J. Colloid Interf. Sci. 181 (1996) 511.
[13] D.J. Durian, Phys. Rev. E 55 (1997) 1739.
[14] T.G. Mason, J. Bibette, D.A. Weitz, Phys. Rev. Lett. 75 (1995) 10.
[15] T.G. Mason, J. Bibette, D.A. Weitz, J. Colloid Interf. Sci. 179 (1996) 439.
[16] T.G. Mason, M.D. Lacasse, G.S. Grest, D. Levine, J. Bibette, D.A. Weitz, Phys. Rev. E 56 (1997) 3150.
[17] M.F. Coughlin, E.P. Ingenito, D. Stamenovic, J. Colloid Interf. Sci. 181 (1996) 661.
[18] S.A. Khan, C.A. Schnepper, R.C. Armstrong, J. Rheol. 32 (1998) 69.
[19] S. Cohen-Addad, H. Hoballah, R. Höhler, Phys. Rev. E 57 (1998) 6897.
[20] A. Saint-Jalmes, D.J. Durian, J. Rheol. 43 (1999) 1411.
[21] T.D. Dimitrova, F. Leal-Calderon, Langmuir 17 (2001) 3235.
[22] L. Bressy, P. Hébraud, V. Schmitt, J. Bibette, Langmuir 19 (2003) 598.
[23] S. Arditty, V. Schmitt, J. Giermanska-Kahn, F. Leal-Calderon, J. Colloid Interf. Sci. 275 (2004) 659.
[24] S.A. Koehler, S. Hilgenfeldt, E.R. Weeks, H. Stone, J. Colloid Interf. Sci. 276 (2004) 439.
[25] A. Saint-Jalmes, Y. Zhang, D. Langevin, Eur. Phys. J. E 15 (2004) 53.
[26] E. Dickinson, Colloid. Surf. B 20 (2001) 197;
E. Dickinson, J. Chem. Soc., Faraday Trans. 94 (1998) 1657.
[27] A.H. Martin, K. Grolle, M.A. Bos, M.A. Cohen Stuart, T. van Vliet, J. Colloid Interf. Sci. 254 (2002) 175.
[28] A. Saint-Jalmes, S. Marze, D. Langevin, in: Eric Dickinson (Ed.), Proceedings of the Food Colloids 2004 Conference: Interactions, Microstructure and Processing, Royal Society of Chemistry, Cambridge, 2004.
[29] L.G. Cascao-Pereira, C. Johanssonn, C.J. Radke, H.W. Blanch, Langmuir 19 (2003) 7503.
[30] A. Saint-Jalmes, H. Ferraz, M. Peugeot, D. Langevin, Colloid Surf. A, doi:10.1016/j.colsurfa.2005.01.014.
[31] S.H. Hilgenfeldt, S.A. Koehler, H.A. Stone, Phys. Rev. Lett. 86 (20) (2001) 4704.
[32] A. Saint-Jalmes, M.U. Vera, D.J. Durian, Eur. Phys. J. B 12 (1999) 67.
[33] H.A. Barnes, J.F. Hutton, K. Walters, An Introduction to Rheology, Elsevier, Amsterdam, 1989.
[34] A.D. Gopal, D.J. Durian, Phys. Rev. Lett. 91 (2003) 188303.
[35] S. Cohen-Addad, R. Höhler, Y. Khidas, Phys. Rev. Lett. 93 (2004) 028302.
[36] D.M.A. Buzza, C.-Y.D. Lu, M.E. Cates, J. Phys. II France 5 (1995) 37.
[37] G. Debrégeas, H. Tabuteau, J.-M. di Meglio, Phys. Rev. Lett. 87 (2001) 17.
[38] P. Coussot, J.S. Raynaud, F. Bertrand, P. Moucheront, J.P. Guilbaud, H.T. Huynh, S. Jarny, D. Lesueur, Phys. Rev. Lett. 88 (2002) 21.
[39] J.-B. Salmon, A. Colin, S. Manneville, F. Molino, Phys. Rev. Lett. 90 (2003) 228303.
[40] A.D. Gopal, D.J. Durian, J. Colloid Interf. Sci. 213 (2002) 169.
[41] B. Herzhaft, J. Colloid Interf. Sci. 247 (2002) 412.
[42] D. Weaire, S. Hutzler, Phil. Mag. 83 (2003) 2747.
[43] R.A. Bagnold, The Physics of Blown Sand and Desert Dunes, Methuen, London, 1941.
[44] S. Hutzler, D. Weaire, R. Crawford, Europhys. Lett. 41 (1998) 461.
[45] M.U. Vera, A. Saint-Jalmes, D.J. Durian, Phys. Rev. Lett. 84 (2001) 3001.